Transformation of nanoporous oxoselenoantimonates into Sb_2O_3—nanoribbons and nanorods

Dorota Sendor,*[a] Thomas Weirich[b] and Ulrich Simon[a]

Received (in Cambridge, UK) 8th July 2005, Accepted 19th September 2005
First published as an Advance Article on the web 20th October 2005
DOI: 10.1039/b509657j

We have isolated flexible Sb_2O_3 nanoribbons and nanorods as the main product from the disintegration of nanoporous oxoselenoantimonates of the cetineite type, the size of the one-dimensional nanomaterials obtained ranging up to 15 μm in length with diameters between 8 and 50 nm.

The fabrication of nanometre-sized one dimensional (1D) inorganic materials has received steadily growing interest in recent years.[1–4] Such 1D structures are objects of intense studies in fundamental chemistry as well as in mesoscopic physics and have opened several technologically relevant applications. Synthetic approaches developed up to now for generating nanostructures with 1D morphologies (wires, rods, belts, and tubes) can be classified into the following three groups, where anisotropic growth is (i) dictated by the linear, crystallographic structure of the solid materials, (ii) directed or confined by a hard or soft template and (iii) kinetically achieved by controlling the super-saturation or by the use of an appropriate capping agent.[4] Nanotubes and nanofibers may carry charge and excitons efficiently, and thus they are promising building blocks for nanoscale electronics[5] and optoelectronics,[6] optically transparent electrodes in light-emitting diodes[7,8] and catalysis.[9] However, another approach has only rarely been used to generate nanostructures in general, namely controlled disassembly of a solid having structural features, like cluster units or linear chains, in order to isolate and to stabilize these subunits.[10] Such an approach would without doubt be beneficial for the chemical synthesis of nanostructures in high yields and can be considered as a SOlid-to-NAnostructure Transformation (SONAT).

We followed this idea by using so called cetineite-type oxoselenoantimonates as a starting material having tubular $Sb_{12}O_{18}$ units as building blocks and succeeded in the formation of μm-sized single-crystalline Sb_2O_3 nanoribbons and nanorods with a diameter ranging from 8–50 nm and with extraordinarily high aspect ratio. Scanning electron microscopy (SEM), high resolution transmission microscopy (HRTEM), powder X-ray diffraction (XRD) and atomic force microscopy (AFM) were used to structurally and morphologically characterise these fibers. Energy dispersive X-ray analysis (EDX) has been employed to analyse the chemical composition..

[a]*Institute of Inorganic Chemistry, RWTH Aachen, Landoltweg 1, Aachen, Germany. E-mail: dorota.sendor@ac.rwth-aachen.de; ulrich.simon@ac.rwth-aachen.de; Fax: +49 241 80 99003; Tel: +49 241 8094644*
[b]*Central Facility for Electron Microscopy, RWTH Aachen, Ahornstrasse 55, Germany. E-mail: weirich@gfe.rwth-aachen.de; Fax: +49 2418022313; Tel: +49 241 8024349*

Sb_2O_3 and Sb_2O_5 nanorods have been already prepared by using a microemulsion method,[11] by hydrothermal conditions,[12] by using carbon nanotubes as the template[13] or by a vapour–solid route.[14] Sb_2O_3 nanobelts and nanotubes have been prepared by surfactant-assisted solvothermal approach.[15]

Cetineites are oxoselenoantimonates with a zeolite-like channel structure, which can be obtained as large single crystals in the range of millimetres from hydrothermal synthesis. The formula of the cetineite described here is $K_6[Sb_{12}O_{18}][SbSe_3]_2 \cdot 6H_2O$.[16] The crystal formula is usually abbreviated as (K;Se). The two main structural characteristics of cetineites are large infinite $Sb_{12}O_{18}$ tubes and isolated $[SbSe_3]^{3-}$ pyramids (see Fig. 1). A tube consists of interconnected SbO_3 pyramids which have a 6_3 axis. The tubes form a two-dimensional hexagonal lattice perpendicular to their axes as is found in ordered arrangements in single-walled carbon nanotubes.[1] The $[SbSe_3]^{3-}$ pyramids are located in the tubular interstices; the plane in which the three Se atoms lie is perpendicular to the tube axes. In a single interstice, infinite in the *c* direction, all pyramids have the same orientation; this orientation, however, varies at random from one interstice to the next. The hexagonal lattice constants (space group space group $P6_3$ or $P6_3/m$) for the cetineite class are 1.41 nm $\leqslant a \leqslant$ 1.46 nm and $c \approx 0.55$ nm; the voids within the tubes have a diameter of approx. 0.7 nm.

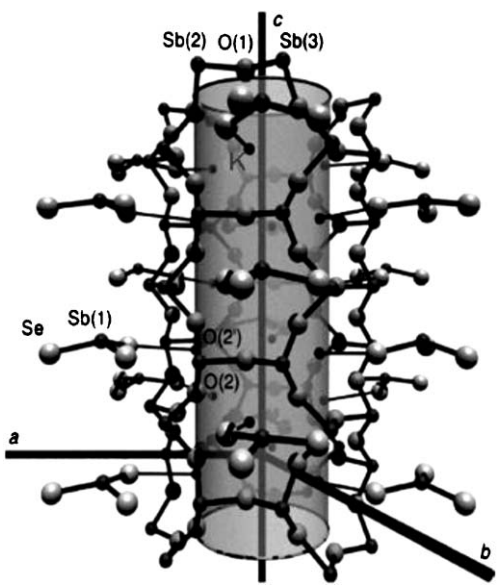

Fig. 1 Structure of the cetineite (K;Se) in perspective into one tube. The shaded tube is included only as a guide for the eye.

 This journal is © The Royal Society of Chemistry 2005

From chemical considerations it is assumed that there are strong Sb–O bonds that stabilise the $Sb_{12}O_{18}$ tubes. The binding among the tubes is thought to be *via* the $[SbSe_3]^{3-}$ pyramids, which are assumed to have ionic bonds to the K^+ ions on the internal wall of the tube and additional weaker bonds to the Sb(2) atoms of the tube wall (see Fig. 1, numbers in parentheses following the atom name denote geometrically nonequivalent atoms of the same species). The host lattice can (and easily does) accept a number of guest molecules. A common guest species is water in connection with a alkali metal. Water molecules can be extracted from the tubes by evacuating the environment and heating the crystals. The electronic structure as well as the electrical and optical properties have been reported in our earlier works.[17]

The structural features lead us to the question whether the $Sb_{12}O_{18}$ channels can be isolated from the compact crystal as a new SbO_x modification.

Cetineites used in this work have been synthesised under hydrothermal condition. In a typical experiment for example (K;Se) 0.38 g Sb, 0.37 g Se and 0.4 g KOH were mixed with 1.3 g H_2O and 0.25 ml 2-aminopentane. The mixture was transferred into a Teflon-coated autoclave and heated at 200 °C for four days, washed with water and dried in air. After this 34 mg of the crystalline product were crushed and placed together with 58 mg 18-crown-6-ether (Fluka 99.5%) and 8.5 ml HCl (0.1 mmol) in a reaction vessel. After mechanically stirring at 800 rpm for two days a milky suspension was obtained, which was twice centrifuged at 8000 rpm for 15 minutes. In the present case the initial characterisation of the products was carried out by powder XRD measurements (CuKα_1, λ = 1.54059 Å) on thin films using the Huber Image Plate in transmission mode. The powder diffraction patterns were analysed using the Stoe WinXPow 1.06 Software package (Stoe & CIE GmbH). All samples gave almost identical patterns with only slightly varying in the peak width. Fig. 2 shows a typical XRD pattern of the material obtained, which illustrates the formation of a single phase compound. However, the XRD lines of the material were broadened indicating nanoscale size (compared to measurement of a SiO_2 standard). The diffraction peaks can be indexed using the matrix of an orthorhombic Sb_2O_3 phase with space group *Pccn*[18] with lattice parameters a = 4.93(1) Å, b = 12.47(8) Å and c = 5.52(3) Å. Refinement calculation of a powder diffraction profile does not indicate any preferred orientation of the sample. The sample morphology was examined by SEM analysis using a Zeiss DSM 982 Gemini. For this purpose, a small amount of the suspension was placed on a Si substrate and kept in a drying oven at 60 °C for one hour. Analysis of the morphology showed changing proportions of (flexible) nanoribbons and nanorods (Fig. 3a, 3b) for the same experimental conditions. However, the SEM images show that entangled and uniform ribbons or rods could be isolated in high yields in all trials. The diameters of the one-dimensional materials range typically from 20 to 50 nm and their lengths are up to 15 μm. Whereas the ribbons/rods appear randomly distributed in water, a pronounced textured material is obtained with MeCN as solvent. This effect is presumably due to hydrophobic interactions between the fibrous material. Based on the morphology of the precursor cetineite we propose the following mechanism for the formation of nanoribbons and nanorods, respectively. The sequence of transformation is likely initiated by addition of HCl which has the effect of removing the antimony selenide groups located at the center of the unit cell. This process is likely accompanied by opening the Sb–O tubes (formation of sheets). Subsequent addition of 18-crown-6-ether removes the potassium cations from the Sb–O sheets which then combine to larger assemblies in order to maintain the charge balance. At present we have no explanation why the reaction leads to formation of two different morphologies (ribbons, rods) with sometimes strikingly different yields under the same experimental conditions. Analysis of the material by energy dispersive X-ray analysis (EDX) indicates that the nanoribbon/rod product consist only of antimony and oxygen with a ratio of about 2 : 3. Specimens for TEM investigation were prepared by air drying the suspension on carbon-coated copper grids. Investigation of the material was carried out in a FEI Tecani F20 electron microscope operated at 200 kV. Detailed analysis of TEM images proves the presence of nanoribbons and nanorods in the samples (Fig. 4). We do not have evidence of any hollow structure in our ribbons and rods. Some TEM images show contrasting tube-like structures. But a detailed analysis clearly indicates that this contrast results from the formation of bundles of nanoribbons and nanorods (Fig. 4). As an example we found assemblies of three nanorods (region C in Fig. 4) as well of only two nanorods (region D in

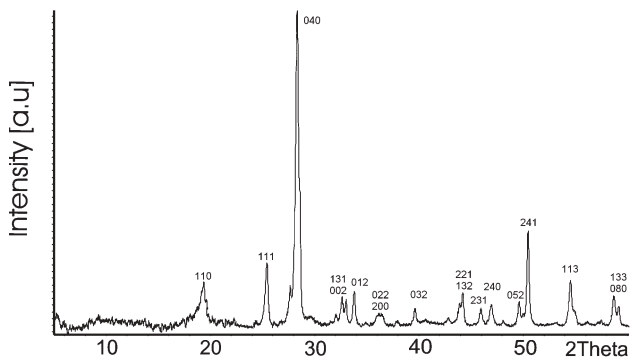

Fig. 2 X-Ray diffraction pattern of Sb_2O_3 nanoribbons.

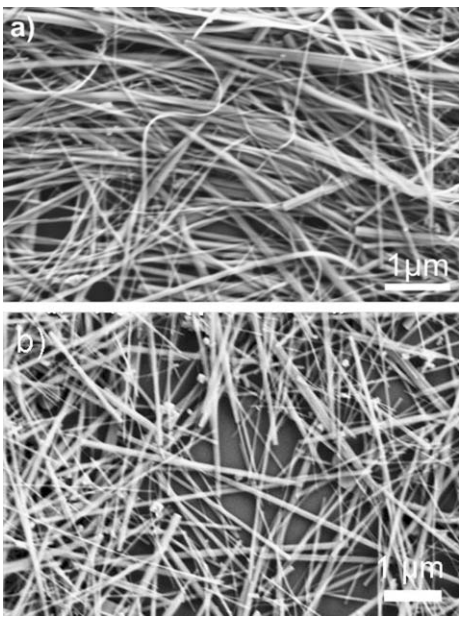

Fig. 3 SEM picture of (a) Sb_2O_3 nanoribbons and (b) Sb_2O_3 nanorods.

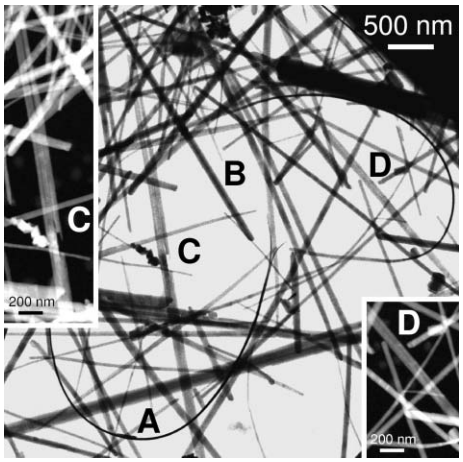

Fig. 4 Bright-field STEM image of Sb_2O_3 nanoribbons (A), nanorods (B) with Z-contrast STEM image as inset Sb_2O_3 nanorods (C, D).

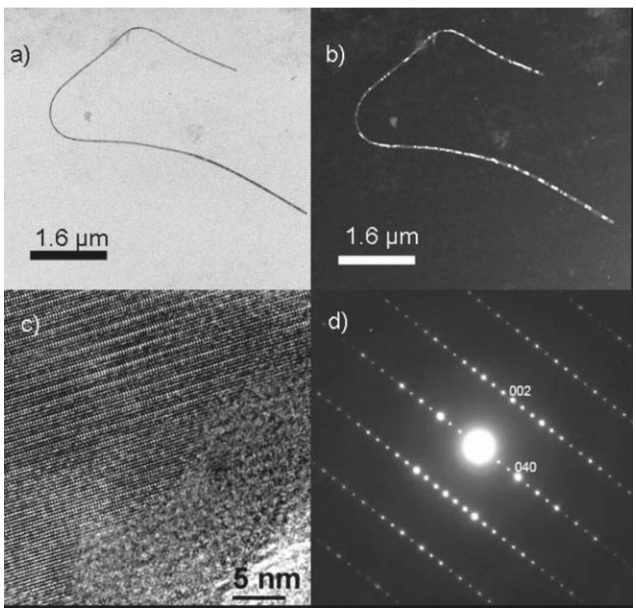

Fig. 5 (a) Bright-field TEM micrograph of individual Sb_2O_3 nanoribbons, (b) dark-field TEM micrograph of individual Sb_2O_3 nanoribbons, (c) HRTEM micrograph of individual Sb_2O_3 nanoribbons with corresponding SAED pattern along the [100] direction (d).

Fig. 4). The latter have similar contrast to the one-dimensional structure reported by Zhang *et al.*[15] and which were interpreted as nanotubes. In particular the non-symmetrical brighter line along the rod axis is a strong argument against this interpretation in terms of a tubular structure in our case.

The Sb_2O_3 nanoribbons and nanorods observed in the present study were sometimes up to 15 μm long with projected diameters in the range between 8 and 50 nm. The thickness of the ribbons is about 15 nm as estimated from TEM/STEM images which show ribbons approximately in side view (Fig. 4, region A). Individual ribbons could be also isolated by diluting the suspension (Fig. 5a). Dark-field imaging (Fig. 5b) indicates that the bent nanoribbons are fully crystalline over the whole length. This result could also be confirmed by high-resolution TEM (Fig. 5c) and by selected area electron diffraction, SAED (Fig. 5d). Measurements by atomic force microscope (AFM) were carried by a Digital Instrument Nanoscope IIIA Multimode AFM measured in tapping mode (tip: Nano World Pointprobe, n+-Silicon). The results obtained indicated that assembly of smaller subunits of these molecular nanorods into thicker bundles takes place. This ability to form bundles might explain the variable diameters observed in SEM and TEM images.

In summary we have developed an approach to synthesize and fabricate nanoribbons and nanorods of orthorhombic Sb_2O_3 as a disintegration process from tubular $Sb_{12}O_{18}$ units, the latter being the fundamental building blocks of cetineites. Characterisation by electron microscopy and XRD show that the obtained nanofibrous material is crystalline. Measurement of the electrical transport properties of individual ribbons/rods are currently under way to explore their potential for use in gas sensors[9] or microelectronic devices.

DS gratefully acknowledges the Alexander von Humboldt Foundation (Roman Herzog Forschungsstipendium) for financial support of this work.

Notes and references

1 S. Iijima, *Nature*, 1991, **354**, 56.
2 G. R. Patzke, F. Krumeich and R. Nesper, *Angew. Chem., Int. Ed.*, 2002, **41**, 2446.
3 G. A. Ozin, *Adv. Mater.*, 1992, **4**, 612.
4 Y. Xia, P. Yang, Y. Sun, Y. Wu, B. Mayers, B. Gates, Y. Yin, F. Kim and H. Yan, *Adv. Mater.*, 2003, **15**, 353.
5 P. D. Yang and C. M. Lieber, *Science*, 1996, **273**, 1836.
6 X. Duan, Y. Huang, Y. Cui, J. Wang and Ch. M. Lieber, *Nature*, 2001, **409**, 66.
7 X. C. Wu, W. H. Song, W. D. Huang, M. H. Pu, B. Zhao, Y. P. Sun and J. J. Du, *Chem. Phys. Lett.*, 2000, **328**, 5; M. H. Huang, S. Mao, H. Feick, H. Yan, Y. Wu, H. Kind, E. Weber, R. Russo, W. Park and G-Ch. Yi, *Adv. Mater.*, 2004, **16**, 87.
8 P. Yang, *Science*, 2001, **292**, 1897; X. C. Wu, W. H. Song, W. D. Huang, M. H. Pu, B. Zhao, Y. P. Sun and J. J. Du, *Chem. Phys. Lett.*, 2000, 328; O. Hayden and A. B. Greytak, *Adv. Mater.*, 2005, **17**, 701.
9 J. Hagen, *Industrial Catalysis*, VCH, 1999; U.-A. Schubert, F. Anderle, J. Spengler, J. Zühlke, H.-J. Eberle, R. K. Grasselli and H. Knözinger, *Top. Catal.*, 2001, **15**, 195; N. Yamazoe, G. Sakai and K. Shimanoe, *Catal. Surv. Asia*, 2003, **7**, 63.
10 M. Schreyer, G. Kraus and T. F. Fässler, *Z. Anorg. Allg. Chem.*, 2004, **630**, 2520.
11 L. Guo, Z. Wu, T. Liu, W. Wang and Z. Zhu, *Chem. Phys. Lett.*, 2000, **318**, 49.
12 X. Chen, X. Wang, Ch. An, J. Liu and Y. Qian, *Mater. Res. Bull.*, 2005, **40**, 469.
13 S. Friedrichs S, R. R. Meyer, J. Sloan, A. I. Kirkland, J. L. Hutchison and M. L. H. Green, *Chem. Commun.*, 2001, 929.
14 Ch. Ye, G. Meng, L. Zhang, G. Wang and Y. Wang, *Chem. Phys. Lett.*, 2002, **363**, 34.
15 Y. Zhang, G. Li, J. Zhang and L. Zhang, *Nanotechnology*, 2004, **15**, 762.
16 X. Wang and F. Liebau, *Eur. J. Solid State Inorg. Chem.*, 1998, **35**, 27; X. Wang and F. Liebau, *Z. Kristallogr.*, 1999, **214**, 820.
17 U. Simon, F. Schüth, S. Schunk, X. Wang and F. Liebau, *Angew. Chem., Int. Ed. Engl.*, 1997, **36**, 1121; F. Starrost, E. Krasowskii, W. Schattke, J. Jockel, U. Simon, R. Adelung, L. Kipp and M. Skibowski, *Phys. Rev. B*, 2000, **61**, 15697; F. Starrost, E. E. Krasovskii, W. Schattke, J. Jockel, U. Simon, X. Wang and F. Liebau, *Phys. Rev. Lett.*, 1998, **80**, 3316; U. Simon, J. Jockel, F. Starrost, E. E. Krasovskii and W. Schattke, *Nanostruct. Mater.*, 1999, **12**, 447.
18 C. Svensson, *Acta Crystallogr., Sect. B: Struct. Crystallogr. Cryst. Chem.*, 1982, **24**, 1968.

 This journal is © The Royal Society of Chemistry 2005